

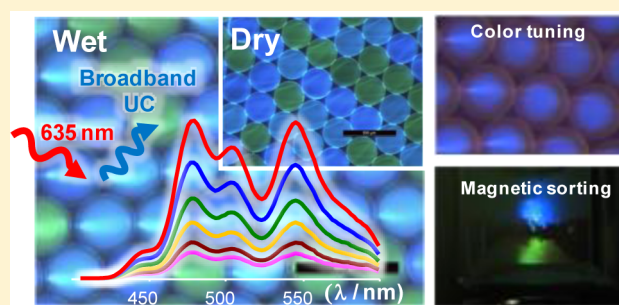
Red-to-Blue/Cyan/Green Upconverting Microcapsules for Aqueous- and Dry-Phase Color Tuning and Magnetic Sorting

Jae-Hyuk Kim,^{†,‡} Fan Deng,[§] Felix N. Castellano,^{*,§} and Jae-Hong Kim^{*,‡}[‡]Department of Chemical and Environmental Engineering, Yale University, New Haven, Connecticut 06511, United States[§]Department of Chemistry, North Carolina State University, Raleigh, North Carolina 27695-8204, United States

S Supporting Information

ABSTRACT: Microcapsules that achieve multicolor triplet–triplet annihilation (TTA)-based upconversion (UC) in both aqueous and dry phases without deoxygenation are presented for the first time. Platinum(II) tetraphenyltetrabenzoporphyrin (PtTPBP) was used as a sensitizer and perylene, 9,10-bis(phenylethynyl)anthracene (BPEA), and a boron dipyrromethene derivative (BD-2) were employed as acceptors for red to blue, cyan, and green UC, respectively. Additional color tuning was introduced into microcapsules by embedding rose bengal onto the microcapsule shell, resulting in UC-mediated excitation of a distal fluorophore through a trivial process. Microcapsules were further modified to host superparamagnetic nanoparticles for magnetic-induced collection, which permitted sorting and color separation potentially instrumental for various photonics-based applications.

KEYWORDS: upconversion, energy transfer, microcapsule, microfluidics, anti-Stokes emission



Photochemical upconversion (UC) is a noncoherent phenomenon wherein the photon energy absorbed by a triplet sensitizer is ultimately emitted from a requisite acceptor, resulting in an anti-Stokes energy shift. In the triplet–triplet annihilation (TTA)-based UC process, triplet sensitization between photoexcited donors and acceptors leads to accumulation of long-lived excited triplet acceptors. This consequently results in TTA between two triplet-excited acceptors, ultimately producing singlet fluorescence characteristic of the acceptor/annihilator. Past studies have been mostly confined to deoxygenated organic solvents to ensure solubility, facile diffusion, and suppression of triplet state dioxygen quenching of the participating chromophores.^{1–8} Several recent studies have explored different media and/or system configurations to overcome these restrictions and expand potential applications. For example, UC has been shown to function in hard and soft polymers,^{9–16} organic/inorganic microparticles/capsules,^{13,17–22} nanocrystalline inorganic films,²³ dendrimers,²⁴ and micelles.²⁵ More recently, UC was shown to efficiently function inside rigid polymeric microcapsules (MCs) of which the inner core consisted of polyisobutylene/hexadecane (PIB/HD) or unsaturated fatty acids and soybean oil,^{13,19} resulting in compositions producing anti-Stokes emission without the need for deoxygenation.

In the current study, several key advances have been made with respect to the previously reported upconverting MCs. The overarching goal here was to significantly expand potential areas of applications such as optical displays, bioimaging, water purification, photovoltaics, and photocatalytic H₂ gas production in both aqueous and dry phases. To achieve multicolor UC

emission (blue, cyan, and green) from a single red excitation source, we employed platinum(II) tetraphenyltetrabenzoporphyrin (PtTPBP) as a sensitizer and perylene, 9,10-bis(phenylethynyl)anthracene (BPEA), and a boron dipyrromethene derivative (BD-2) as acceptors. Three different MCs were fabricated using this sensitizer and each acceptor, yielding distinct emission colors (B, C, or G) from the individual MCs, which are easily combined affording a panchromatic emission response. Additional facile color tuning was introduced into each microcapsule by simply embedding rose bengal (RB) onto the MC shell, resulting in UC-mediated excitation of a distal fluorophore through a trivial process. Finally, superparamagnetic Fe₃O₄ nanoparticles (MNPs) were embedded in select microcapsules, wherein exposure to an external magnet afforded a simple mechanism for magnetic-induced collection, sorting, and color separation of the mixed UC-MC composition. The ability to sort and separate upconverting microspheres appears well poised for a broad range of photonic applications in both aqueous and dry phases.

RESULTS AND DISCUSSION

Preparation of UC Solutions. Three sensitizer/acceptor pairs, PtTPBP as a sensitizer, and perylene, BPEA, and BD-2 as acceptors, were selected to fulfill the energy requirements for TTA-UC, that is, $E(^3\text{Sens}^*) > E(^3\text{Acc}^*)$, $2E(^3\text{Acc}^*) > E(^1\text{Acc}^*)$. The triplet energy state of PtTPBP, perylene, BPEA, and BD-2 are 1.61,²⁶ 1.53,²⁷ 1.53,⁹ and 1.6 eV,²⁸

Received: January 28, 2014

Published: March 5, 2014

respectively. The absorption and emission spectra of the sensitizer and acceptors/annihilators used in this study are shown in Figure 1 along with their molecular structures. The

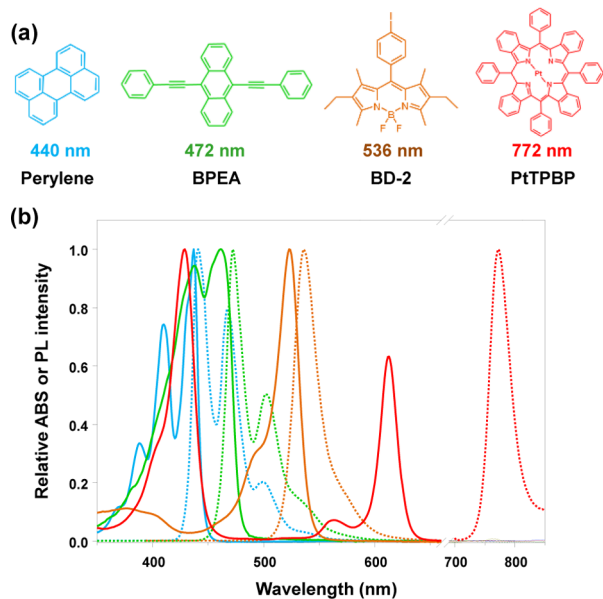


Figure 1. (a) Molecular structure of acceptors and PtTPBP. (b) Normalized absorption (solid lines) and emission (dotted lines) spectra of PtTPBP (red), perylene (light blue), BPEA (green), and BD-2 (brown) in THF at room temperature. For the measurement of phosphorescence of PtTPBP, the solution was deoxygenated by purging with nitrogen gas for 20 min.

wavelength at the highest Stokes emission intensity is also depicted in Figure 1a. Please note that while BD-2 contains iodo-functionality, this imparts no significant influence to the singlet fluorescence properties of this BODIPY dye and it does not serve as an internal heavy atom since it is largely decoupled from the chromophoric species. It was selected for use here, since we had it available as a synthon from a completely unrelated study. Mineral oil (MO) was employed as a host medium, advantageous for its low cost, high boiling point, optical clarity, low dioxygen solubility, and thermal stability. PIB was added to MO, providing a local oxygen depleted environment, thus enabling facile UC without the need for degassing. Liu et al. postulated that the fatty acids present in soybean oil might provide a reductive environment resulting in the depletion of singlet oxygen.¹⁹ Likewise, it is possible that unsaturated double bonds that remain from incomplete polymerization of isobutylene with isoprene participates in sequestering any photochemically produced singlet oxygen (mainly through the ene-reaction). The optimal concentration of PIB was evaluated to be 3.8 wt % by measuring the phosphorescence intensity of PtTPBP (Figure S1) and under these conditions we could not detect the sensitization of ¹O₂ phosphorescence in the near-IR (1270 nm).²⁶ Indirect evidence, namely, a short induction period (~1 min) to reach the maximum stable UC intensity after laser irradiation, suggests that a finite time period is needed to deplete residual molecular oxygen in the composition (data not shown).

Photoluminescence Properties of UC Solutions. The quantum yield (QY) of UC was highly dependent on the acceptor concentration as shown in Figure S2. At the highest acceptor concentration employed in this study, we observed

reproducible UC-QY of 5.3 ($\pm 0.05\%$), 3.3 ($\pm 0.03\%$), and 1.8% ($\pm 0.02\%$) for perylene, BPEA, and BD-2, respectively. The QY was also highly dependent on the incident laser power but did not plateau even at the highest laser power employed in this study, as shown in Figure 2a. Accordingly, when normalized

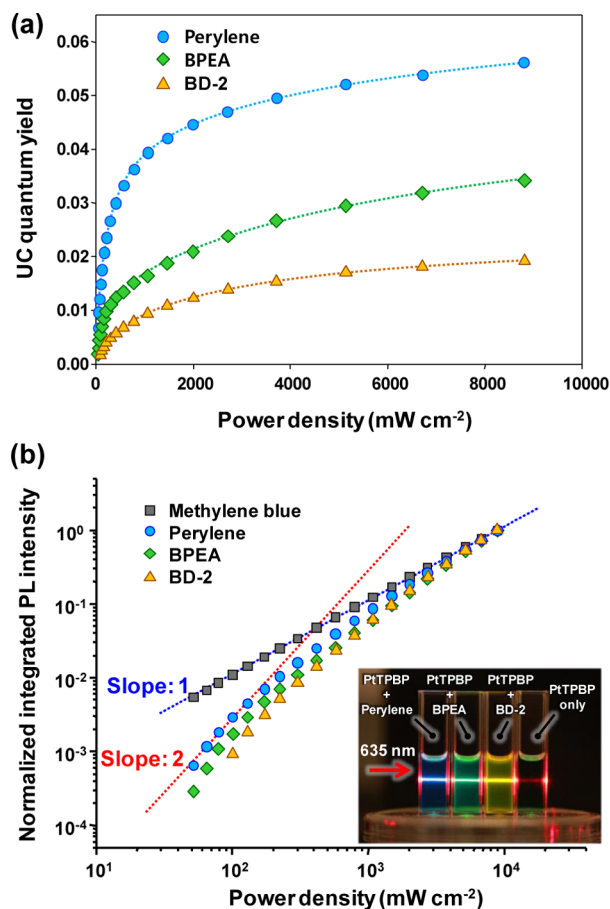


Figure 2. (a) Upconversion quantum yield and (b) normalized integrated emission intensity of PtTPBP/acceptor in PIB/MO as a function of the power density of the incident laser (635 nm). The dashed lines in (b) are the linear fits with slopes of 1.0 (blue, linear) and 2.0 (red, quadratic). Inset in (b) presents digital photograph of the PtTPBP solution in PIB/MO containing different acceptors irradiated by a red laser ($\lambda = 635$ nm). [PtTPBP]: 11 μ M, [perylene]: 1.4 mM, [BPEA]: 1.3 mM, [BD-2]: 1.4 mM.

integrated UC intensity was plotted versus incident power density on double logarithmic scales (Figure 2b), the slope gradually changed from quadratic toward linear but did not achieve linear response. For comparison, the integrated intensity of a standard dye, methylene blue, exhibited a linear excitation power dependence for its nominal fluorescence response. As reported in many recent studies, the UC intensity typically exhibits a transition from quadratic to linear or pseudolinear laser power dependence, at which point triplet excited acceptors are efficiently consumed by participating in TTA rather than unimolecular and pseudo-first order quenching decay pathways.^{8,13,14,19,21,29} Here, this quadratic-to-linear transition starts at approximately at 130, 170, and 300 mW cm^{-2} for perylene, BPEA, and BD-2, respectively. The linear response was not achieved even beyond these power densities presumably due to the relatively high viscosity of mineral oil that hinders effective chromophore diffusion and the

less solubility of acceptors in mineral oil compared to other commonly used solvents. A typical emission intensity dependence profile of the UC solutions measured as a function of incident excitation power is presented in Figure S3. We observed that the bulk PtTPBP/acceptor solutions in PIB/MO displayed intense UC emission from monochromatic red excitation at 635 nm (see inset in Figure 2b). Note that the UC emission from the bulk solutions more closely resemble blue/green/yellow, likely due to the strong self-absorption of upconverted photons by the analogous acceptor molecules present in large concentration.

Preparation and Photoluminescence Properties of the UC Microcapsules. The MCs that encapsulate the MO/PIB phase were fabricated using a glass capillary microfluidic device.¹³ Two immiscible oil phases, PIB/MO and photocurable polymer mixture (ethoxylated-trimethylolpropanetriacrylate esters, ETPTA), were flowed in the lower and upper channel of theta (θ)-shaped capillary glass, respectively, and emulsified in an aqueous continuous phase containing surfactant (polyvinyl alcohol) to form oil-in-oil-in-water (o/o/w) double emulsion droplets. The ETPTA polymer phase completely dewetted the surface of PIB/MO due to the hydrophobicity of PIB/MO and relative hydrophilicity of ETPTA. The ETPTA phase was then rapidly solidified using UV irradiation yielding a cross-linked rigid polymer shell. Figure S4 shows the optical microscope image taken at the junction part of the capillary glasses during double emulsion droplets generation. Even after sequential washing steps to completely remove the residual surfactant, the MCs dispersed in surfactant-free water without any noticeable agglomeration. The MCs with the PIB/MO core containing PtTPBP/perylene, PtTPBP/BPEA, and PtTPBP/BD-2 are referred to herein as MC_{PER} , MC_{BPEA} , and MC_{BD2} , respectively.

The prepared MCs were spherical and highly uniform with average diameter of 280 μm . Figure S5 displays a clear hollow inner space after releasing the PIB/MO phase through intentional breakage of the shell. Figures 3a–h and S6 presents microscope images and the associated anti-Stokes emission spectra of the prepared MCs in water under monochromatic excitation at 635 nm. The intense upconverted blue, cyan, and yellowish-green emissions were clearly observed from the core of the MC_{PER} , MC_{BPEA} , and MC_{BD2} , respectively, when visualized through a 600 nm short-pass filter. The upconverted photoluminescence from the MCs dispersed in water was readily observed by the naked eye in the laboratory ambient (insets in Figure 3b,d,f). Due to entrapped PtTPBP in the ETPTA phase, porphyrin-based phosphorescence was also evident (Figure S7), as observed previously.¹³ These UC MCs were found to be photostable when exposed to continuous 635 nm laser irradiation below 160 mW cm^{-2} (Figure S8). At higher laser power irradiance, some photodegradation was evident for MC_{BPEA} and MC_{BD2} (31 and 43%, respectively, after 10 min at 320 mW cm^{-2}), but MC_{PER} exhibited a remarkably high photostability up to 320 mW cm^{-2} of 635 nm excitation power.

The MCs were readily dried in air and deposited onto glass slides as presented in Figure 4. The MCs tend to be closely packed as the water evaporates, eventually forming a hexagonally arranged monolayer. When selectively excited at 635 nm, the blue, cyan, and yellowish-green UC emissions from these dried MCs were clearly observed from the MC_{PER} , MC_{BPEA} , and MC_{BD2} , respectively. These MCs continued to upconvert photons even after 3 months of storage under

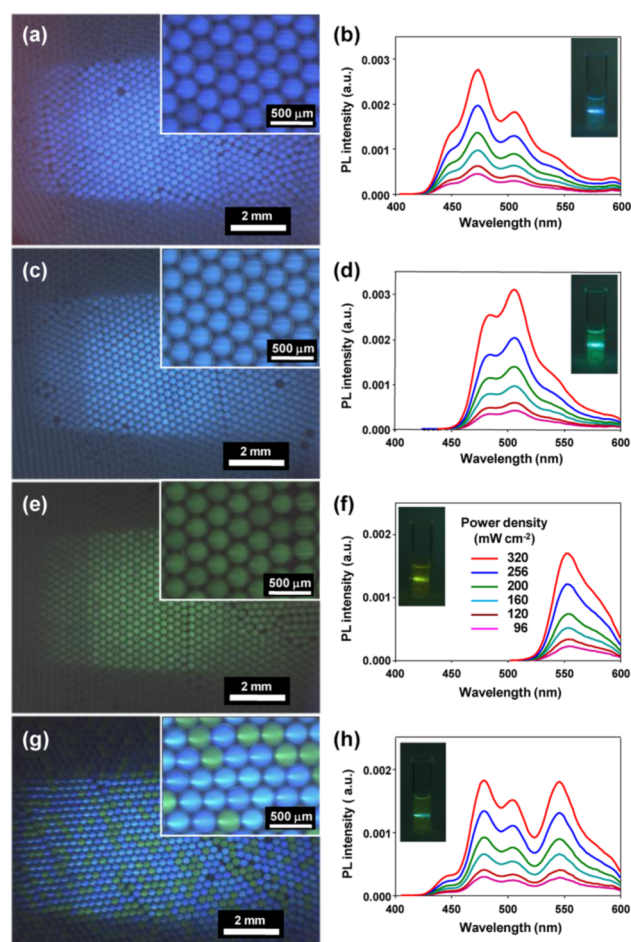


Figure 3. Microscope images and emission profiles of (a, b) MC_{PER} , (c, d) MC_{BPEA} , (e, f) MC_{BD2} , and (g, h) the mixture of MC_{PER} , MC_{BPEA} , and MC_{BD2} in water under the selective excitation at 635 nm. Images were taken through 600 nm short-pass filter. The power density presented in (f) is also applied to all the other spectroscopic measurement. The laser power in (a), (c), (e), and (g) is 200 mW cm^{-2} .

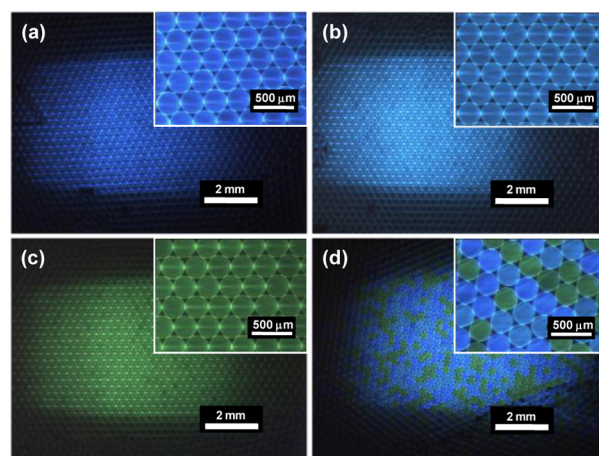


Figure 4. Microscope images of the (a) MC_{PER} , (b) MC_{BPEA} , (c) MC_{BD2} , and (d) mixture of three MCs arrayed and dried on a slide glass under the selective excitation at 635 nm. Images were taken through 600 nm short-pass filter. Laser power: $\sim 200 \text{ mW cm}^{-2}$.

ambient conditions. This dry surface packing of UC materials present a significant advance from past approaches to integrate

TTA-UC with photovoltaics in which sealing the UC media from the ambient represented a major challenge in the system design.^{30,31}

Broadband UC Emission from Mixed MCs Suspensions. The MCs prepared herein represent the first examples of photochemical upconverting soft materials that function in both aqueous and “dry” conditions in oxygen-rich environments. These water-, air-stable, and photo-stable MCs can be further manipulated or decorated to have specific functionality that expands the applicability of this material. First, we were able to achieve broadband UC emission induced through monochromatic (red, 635 nm) excitation by mixing the MCs in appropriate proportions (Figure 3h). Figure S9 presents the UC emission spectra of suspensions containing MC_{PER}/MC_{BPEA} and the MC_{PER}/MC_{BPEA}/MC_{BD2} at different ratios under 635 nm illumination. As the volumetric portion of the MC_{BPEA} increases, the spectrum resembled that of the single MC_{BPEA} suspension, Figure S9a. Similar observations were made when the three MCs were combined. Interestingly, even when MC_{BD2} constituted a minor fraction of the mixture (<2.5 vol %), there was a drastic increase of emission near 540 nm corresponding to BD-2 fluorescence, accompanied by a significant decrease of the UC intensity between 470–510 nm (Figure S9b). Considering that the BD-2 emission of the mixed MCs (<2.5 vol%) was clearly blue-shifted (λ_{\max} : 540 nm) compared to that from the MC_{BD2} alone (λ_{\max} : 552 nm, Figure 3f) and that the BD-2 absorption overlaps the MC_{PER}/MC_{BPEA} emissions, we believe that the upconverted photons generated from the MC_{PER} and MC_{BPEA} sensitized BD-2 fluorescence in the core of MC_{BD2} through the trivial mechanism (i.e., simple absorption of the upconverted fluorescence). With increasing volumetric portion of MC_{BD2}, the UC intensity at 550 nm gradually increased, achieving a maximum at 33 vol %. Over this titration, the BD-2 fluorescence eventually red-shifted, mostly due to the self-absorption by the increased amount of surrounding MC_{BD2}, indicating that UC sensitization became solely responsible for this fluorescence. These observations are significant as only a handful of studies have demonstrated white light emission using single pairs of donor/acceptor in solutions.^{32–34}

Emission Color Tuning of MCs by Selective Embedding Secondary Dye in the Polymer Shell. Second, inspired by the above result, UC-mediated color-tunable microcapsules were prepared by embedding RB into the shell of the MC_{PER}, coded as MC_{RB}, as schematically shown in Figure 5a. This is based on the sensitization of a secondary fluorophore (RB) present in the MC shell by upconverted photons produced in the core. Note that the RB absorptions range from 400 to 600 nm (Figure S10), overlapping well with the perylene fluorescence but not resonant with the laser excitation (635 nm). Also note that RB does not participate in the UC process with PtTPBP, since its triplet energy state does not fulfill the proper energy criteria ($E(^3\text{PtTPBP}^*) = 1.61 \text{ eV} < E(^3\text{RB}^*) = 1.77 \text{ eV}$).^{26,35} Color tuning was achieved by precisely controlling the thickness of the RB-containing shell. The flow rate ratio of PIB/MO and RB-containing ETPTA was precisely adjusted while the overall MC diameter was maintained constant (inset in Figure 5b–e). Figure 5f presents the emission profiles of MCs with different core/shell volume ratios. Despite the fact that the fluorescence QY of RB is relatively low (<11%) and the RB-containing shell is very thin (<10 nm), a substantial amount of RB fluorescence at 580 nm was clearly detected along with upconverted photons. As the

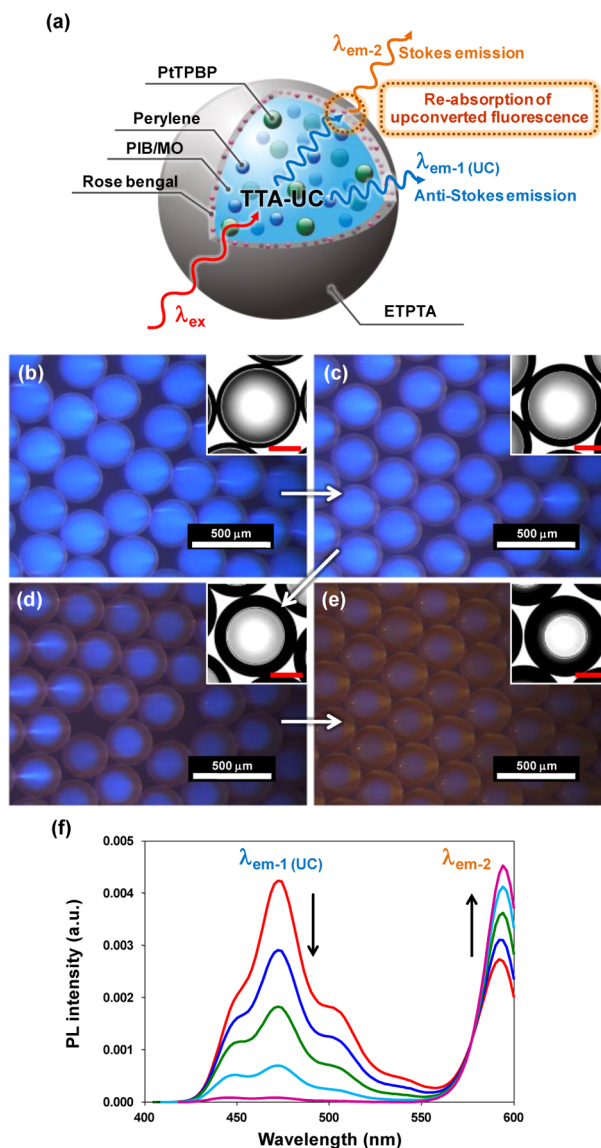


Figure 5. (a) Schematic illustration of the MC_{RB}. (b–e) Microscope images and (f) emission profiles of the MC_{RB} in water with different core–shell volume ratio under the selective excitation at 635 nm. Optical microscope images obtained under white-light illumination are presented in (b–e) as insets (scale bar: 100 μm) to show shell thickness changes as well as clear boundary between inner phase and shell. Arrows in (b–f) indicate shell thickness increase.

shell thickness increased and the core volume decreased, the anti-Stokes emission from the core phase decreased significantly due to increased absorption via RB in the shell. Even though the upconverting core became smaller, the UC emission intensity was sufficient to induce RB fluorescence. As the shell became thicker, the overall emission from the MC, that is, the sum of UC anti-Stokes emission and RB fluorescence, changed from blue to yellow-orange, as shown in Figures 5b–e and S11. Additionally, the photoluminescence of MC_{RB} was notably stable (Figure S12), as it was produced from the PtTPBP/perylene core as mentioned above. The approach of indirectly sensitizing a dye through upconverted photons presents a unique way for emission color tuning in soft materials hosting photochemical UC. For example, by combining all the MCs prepared in this study (MC_{PER}, MC_{BPEA}, MC_{BD2}, MC_{RB}), we

obtained panchromatic emission under monochromatic excitation at 635 nm (Figure 6).

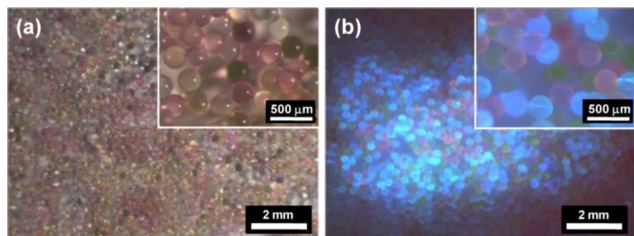


Figure 6. Microscope images of the mixture of MC_{PER} , MC_{BPEA} , MC_{BD2} , and MC_{RB} filtered and dried on the filter disk (a) under white light illumination and (b) under the irradiation of 635 nm laser and (b) was taken through 600 nm short-pass filter.

Magnetic Separation of MCs from Mixed Suspensions. Third, paramagnetism can be incorporated into these MCs rendering them separable through exposure to a magnet for various color-sorting applications, recovery purposes, and site-specific visualization, particularly advantageous for applications in bioimaging. As a proof-of-concept example, we embedded iron oxide (Fe_3O_4) MNPs into the shell of MC_{BD2} spheres. The MNPs reduced the UC emission by $\sim 34\%$ due to absorption and scattering, but the UC photoluminescence remained discernible by the naked eye (Figure S13). Figure 7

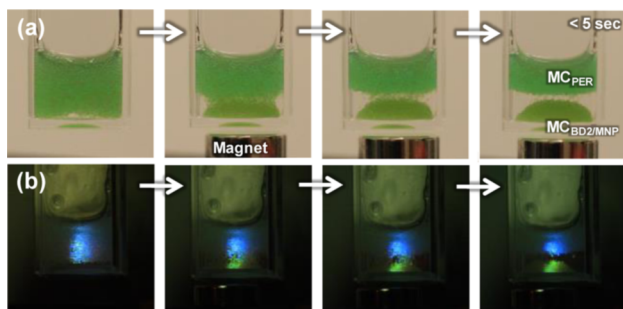


Figure 7. Digital photographs of time-courses separation of mixed MCs of $MC_{BD2/MNP}$ and MC_{PER} by applying magnetic field (a) without and (b) with laser irradiation at 635 nm. Image (b) was taken through 600 nm short-pass filter. NaCl was added to the water to adjust the buoyancy of the MCs so that they readily suspended in water in the absence of the magnetic field.

presents time-course photographs taken during the magnetic separation of $MC_{BD2/MNP}$ from MC_{PER} . Within a few seconds, $MC_{BD2/MNP}$ were collected at the bottom of the vial resulting from exposure to a permanent magnet while MC_{PER} remained suspended in water such that its characteristic green fluorescence was easily discernible from the blue emission in each of the spheres. We confirmed that the MCs exhibited quantitatively similar emission profiles and intensities compared to that before exposure to the permanent magnet. These results represent the first example where distinct UC emitting compositions have been combined and separated in a facile manner.

CONCLUSIONS

In conclusion, this study demonstrates the first color-tunable and magnetically separable red-to-blue/cyan/green upconverting MCs that function both in aqueous and dry phases. PtTPBP

paired with perylene, BPEA, and BD-2, dissolved in PIB/MO enabled UC with moderate to high upconversion quantum yields (1.6–5.6%) in oxygen-rich environments. Combined with the ability to indirectly sensitize a fluorophore using trivial energy transfer, the present soft material design affords color tuning as well as broadband emission from a monochromatic light source. Facile magnetic separation also allows UC substrate retrieval particularly suitable for bioimaging and related applications in photonics.

EXPERIMENTAL METHODS

Preparation of Upconversion Media. PIB (MW: ~ 1350 , Polyscience Inc.) at 3.8 wt % was added to light MO (Aldrich) to prepare the UC medium (PIB/MO). An aliquot of tetrahydrofuran (THF) containing PtTPBP (Frontier Scientific), perylene (Aldrich), BPEA (Aldrich), and BD-2 (synthesized as ref 1) was added to PIB/MO. The solution was then placed in a convection oven at $70^\circ C$ for more than 12 h to completely evaporate THF.

Microfluidic Device. A primary glass capillary (World Precision Instruments, TST150–6) with a theta (θ) shape was tapered using a micropipet puller (Sutter Instrument, P-97), cut after scoring with a ceramic tile (Sutter Instrument, FG-CTS), and inserted in a secondary glass tube (I.D. = 1.56 mm, Sutter Instrument, BF200–156–10). The inner diameter of the tip was typically about $100\ \mu m$. The another glass capillary tube (I.D. = 0.84 mm, World Precision Instruments, 1B150–6) was also tapered (I.D. = c.a. $280\ \mu m$) and treated with 2-[methoxy(polyethyleneoxy)propyl] trimethoxysilane (Gelest Inc.) in toluene to render the inner surface hydrophilic. Then it was inserted into the secondary glass tube in an opposite direction and carefully aligned with the primary glass capillary. An aqueous solution (1 wt %) of polyvinyl alcohol (PVA, Mowiol 4–88, MW: ~ 31000 , Aldrich) was used as a continuous phase. The polymer phase was prepared by mixing 4 mL of ETPTA (SR454, Sartomer Inc.) with photoinitiator (Irgacure 2100, $150\ \mu L$, BASF Chemicals), amine acrylate co-initiator (CN373, $100\ \mu L$, Sartomer, Inc.), and benzophenone (0.53 M in THF, $50\ \mu L$, Aldrich). To prepare dye- or MNP-embedded microcapsule shell, an aliquot of RB (4.9 mM in THF, $150\ \mu L$, Aldrich) or MNP in toluene ($200\ \mu L$, Aldrich) was further added to the ETPTA mixture, sonicated, and subsequently placed in the oven at $70^\circ C$ for more than 12 h to evaporate solvent. The polymer phase and PIB/MO solvent phase flowed separately in each channel of the primary glass capillary. Typically, the flow rate of the polymer phase, solvent phase, and continuous phase were 11.3 , 7.5 , and $600\ \mu L\ min^{-1}$, respectively, and controlled using syringe pumps (Harvard Apparatus). The fabricated microcapsule was cured using UV lamp (100 W, Upland) and two black lamp bulbs (BLB, 4 W) simultaneously and collected in a PVA solution (1 wt %) under gentle stirring. The microcapsules were further treated in a photoreactor equipped with five BLB lamps (4 W) for 2 min for the curing of residual unreacted polymer, collected after filtering with $0.45\ \mu m$ filter (Supor-450, PALL Life Sciences), washed with copious amounts of distilled water, and stored in a deionized water.

Spectroscopic Measurements. The static absorption spectra and Stokes emission spectra of the chromophore solution were analyzed on a UV–visible spectrophotometer (Agilent 8453) and spectrofluorometer (Shimadzu, RF-5301), respectively. Stokes and Antistokes emission spectra of the UC solutions were obtained with a commercial diode laser (635

nm) as the excitation source. Emission from the solution in cuvette was collected normal to excitation and passed through a series of focusing lenses and an optical chopper (120 Hz) before reaching a monochromator (Oriel Cornerstone, Newport Corp.). For the measurement of emission from the MCs, the laser beam was irradiated to a cuvette containing precipitated MCs in water at an approximate 40° angle. Incident laser power was adjusted through the use of a series of neutral density filters and was measured using a Nova II power meter/photodiode detector head (Ophir). The signal was detected by an Oriel photomultiplier tube and processed by an Oriel Merlin radiometry detection system (Newport Corp.). The sensitized upconverted fluorescence quantum yield measurements of perylene, BPEA, and BD-2 in PIB/MO were measured relative to methylene blue in methanol using a 635 nm diode laser, utilizing the following equation:³⁶

$$\Phi_{UC} = 2\Phi_{std} \left(\frac{A_{std}}{A_{UC}} \right) \left(\frac{I_{UC}}{I_{std}} \right) \left(\frac{\eta_{UC}}{\eta_{std}} \right)^2 \quad (1)$$

where Φ_{UC} , A_{UC} , I_{UC} , and η_{UC} represents the quantum yield, absorbance, integrated photoluminescence intensity, and refractive index of the upconversion sample at the excitation wavelength. The corresponding terms for the subscript “std” are for the reference quantum counter at the corresponding excitation wavelength. The QY standard was methylene blue in methanol, whose $\Phi_{std} = 0.03$.³⁷ The refractive index of the solvents used were $\eta_{MeOH} = 1.329$ and $\eta_{MO} = 1.467$, as obtained from Sigma-Aldrich solvent physical properties. The integrated intensities of the upconverted fluorescence were analyzed in the region 400–600 nm (perylene), 450–600 nm (BPEA), and 490–600 nm (BD-2), while that of methylene blue was analyzed in the region 600–850 nm.

■ ASSOCIATED CONTENT

● Supporting Information

Microscope images of the microfluidic device or various MCs with or without 635 nm excitation, optimization of PIB concentration in MO, quantum yield and emission profile as a function acceptor concentration, wide range emission profile of MCs, UC emission intensity of various MCs along with irradiation time and power, emission profile of the mixed MCs, molecular structure, absorption and emission spectra of rose bengal, and comparison of emission profiles of MC_{BD2} with and without MNP in the shell. This material is available free of charge via the Internet at <http://pubs.acs.org>.

■ AUTHOR INFORMATION

Corresponding Authors

*E-mail: fncastel@ncsu.edu.

*E-mail: jaehong.kim@yale.edu.

Present Address

[†]School of Civil and Environmental Engineering, Pusan National University, Busan, 609-735, Republic of Korea.

Notes

The authors declare no competing financial interest.

■ ACKNOWLEDGMENTS

This work was partly supported by the National Science Foundation (CBET-1033866 to J.K.), the Korea Institute for Advancement of Technology (2011-GU-400115-001 to J.K.), and the Air Force Office of Scientific Research (FA9550-13-1-

0106 to F.N.C.). F.D. was supported as a Delta Electronics Fellow.

■ REFERENCES

- (1) Singh-Rachford, T. N.; Haefele, A.; Ziesel, R.; Castellano, F. N. Boron Dipyrromethene Chromophores: Next Generation Triplet Acceptors/Annihilators for Low Power Upconversion Schemes. *J. Am. Chem. Soc.* **2008**, *130*, 16164–16165.
- (2) Sugunan, S. K.; Tripathy, U.; Brunet, S. M. K.; Paige, M. F.; Steer, R. P. Mechanisms of Low-Power Noncoherent Photon Upconversion in Metalloporphyrin-Organic Blue Emitter Systems in Solution. *J. Phys. Chem. A* **2009**, *113*, 8548–8556.
- (3) Singh-Rachford, T. N.; Nayak, A.; Muro-Small, M. L.; Goeb, S.; Therien, M. J.; Castellano, F. N. Supermolecular-Chromophore-Sensitized Near-Infrared-to-Visible Photon Upconversion. *J. Am. Chem. Soc.* **2010**, *132*, 14203–14211.
- (4) Cheng, Y. Y.; Fuckel, B.; Khoury, T.; Clady, R.; Tayebjee, M. J. Y.; Ekins-Daukes, N. J.; Crossley, M. J.; Schmidt, T. W. Kinetic Analysis of Photochemical Upconversion by Triplet-Triplet Annihilation: Beyond Any Spin Statistical Limit. *J. Phys. Chem. Lett.* **2010**, *1*, 1795–1799.
- (5) Cheng, Y. Y.; Khoury, T.; Clady, R.; Tayebjee, M. J. Y.; Ekins-Daukes, N. J.; Crossley, M. J.; Schmidt, T. W. On the Efficiency Limit of Triplet-Triplet Annihilation for Photochemical Upconversion. *Phys. Chem. Chem. Phys.* **2010**, *12*, 66–71.
- (6) Singh-Rachford, T. N.; C.; Castellano, F. N. Photon Upconversion Based on Sensitized Triplet-Triplet Annihilation. *Coord. Chem. Rev.* **2010**, *254*, 2560–2573.
- (7) Zhao, J.; Ji, S.; Guo, H. Triplet-Triplet Annihilation Based Upconversion: From Triplet Sensitizers and Triplet Acceptors to Upconversion Quantum Yields. *RSC Adv.* **2011**, *1*, 937–950.
- (8) Haefele, A.; Blumhoff, J.; Khnazyer, R. S.; Castellano, F. N. Getting to the (Square) Root of the Problem: How to Make Noncoherent Pumped Upconversion Linear. *J. Phys. Chem. Lett.* **2012**, *3*, 299–303.
- (9) Monguzzi, A.; Tubino, R.; Meinardi, F. Multicomponent Polymeric Film for Red to Green Low Power Sensitized Upconversion. *J. Phys. Chem. A* **2009**, *113*, 1171–1174.
- (10) Miteva, T.; Yakutkin, V.; Nelles, G.; Balushev, S. Annihilation Assisted Upconversion: All-Organic, Flexible and Transparent Multicolour Display. *New J. Phys.* **2008**, *10*, 103002.
- (11) Singh-Rachford, T. N.; Lott, J.; Weder, C.; Castellano, F. N. Influence of Temperature on Low-Power Upconversion in Rubbery Polymer Blends. *J. Am. Chem. Soc.* **2009**, *131*, 12007–12014.
- (12) Singh-Rachford, T. N.; Castellano, F. N. Triplet Sensitized Red-to-Blue Photon Upconversion. *J. Phys. Chem. Lett.* **2010**, *1*, 195–200.
- (13) Kim, J. H.; Kim, J. H. Encapsulated Triplet-Triplet Annihilation-Based Upconversion in the Aqueous Phase for Sub-Band-Gap Semiconductor Photocatalysis. *J. Am. Chem. Soc.* **2012**, *134*, 17478–17481.
- (14) Jankus, V.; Snedden, E. W.; Bright, D. W.; Whittle, V. L.; Williams, J. A. G.; Monkman, A. Energy Upconversion via Triplet Fusion in Super Yellow PPV Films Doped with Palladium Tetrphenyltetrabenzoporphyrin: A Comprehensive Investigation of Exciton Dynamics. *Adv. Funct. Mater.* **2013**, *23*, 384–393.
- (15) Wohnhaas, C.; Friedemann, K.; Busko, D.; Landfester, K.; Balushev, S.; Crespy, D.; Turshatov, A. All Organic Nanofibers as Ultraviolet Support for Triplet-Triplet Annihilation Upconversion. *ACS Macro Lett.* **2013**, *2*, 446–450.
- (16) Islangulov, R. R.; Lott, J.; Weder, C.; Castellano, F. N. Noncoherent Low-Power Upconversion in Solid Polymer Films. *J. Am. Chem. Soc.* **2007**, *129*, 12652–12653.
- (17) Zhang, C.; Zheng, J. Y.; Zhao, Y. S.; Yao, J. N. Organic Core-Shell Nanostructures: Microemulsion Synthesis and Upconverted Emission. *Chem. Commun.* **2010**, *46*, 4959–4961.
- (18) Wohnhaas, C.; Turshatov, A.; Mailander, V.; Lorenz, S.; Balushev, S.; Miteva, T.; Landfester, K. Annihilation Upconversion in Cells by Embedding the Dye System in Polymeric Nanocapsules. *Macromol. Biosci.* **2011**, *11*, 772–778.

(19) Liu, Q.; Yin, B. R.; Yang, T. S.; Yang, Y. C.; Shen, Z.; Yao, P.; Li, F. Y. A General Strategy for Biocompatible, High-Effective Upconversion Nanocapsules Based on Triplet-Triplet Annihilation. *J. Am. Chem. Soc.* **2013**, *135*, 5029–5037.

(20) Liu, Q.; Yang, T. S.; Feng, W.; Li, F. Y. Blue-Emissive Upconversion Nanoparticles for Low-Power-Excited Bioimaging in Vivo. *J. Am. Chem. Soc.* **2012**, *134*, 5390–5397.

(21) Monguzzi, A.; Frigoli, M.; Larpent, C.; Tubino, R.; Meinardi, F. Low-Power-Photon Up-Conversion in Dual-Dye-Loaded Polymer Nanoparticles. *Adv. Funct. Mater.* **2012**, *22*, 139–143.

(22) Kang, J. H.; Reichmanis, E. Low-Threshold Photon Upconversion Capsules Obtained by Photoinduced Interfacial Polymerization. *Angew. Chem., Int. Ed.* **2012**, *51*, 11841–11844.

(23) Lissau, J. S.; Gardner, J. M.; Morandeira, A. Photon Upconversion on Dye-Sensitized Nanostructured ZrO₂ Films. *J. Phys. Chem. C* **2011**, *115*, 23226–23232.

(24) Tanaka, K.; Inafuku, K.; Chujo, Y. Environment-Responsive Upconversion Based on Dendrimer-Supported Efficient Triplet-Triplet Annihilation in Aqueous Media. *Chem. Commun.* **2010**, *46*, 4378–4380.

(25) Turshatov, A.; Busko, D.; Balushev, S.; Miteva, T.; Landfester, K. Micellar Carrier for Triplet-Triplet Annihilation-Assisted Photon Energy Upconversion in a Water Environment. *New J. Phys.* **2011**, *13*, 083035.

(26) Singh-Rachford, T. N.; Castellano, F. N. Supra-Nanosecond Dynamics of a Red-to-Blue Photon Upconversion System. *Inorg. Chem.* **2009**, *48*, 2541–2548.

(27) Chen, Y. H.; Zhao, J. Z.; Xie, L. J.; Guo, H. M.; Li, Q. T. Thienyl-Substituted Bodipys with Strong Visible Light-Absorption and Long-Lived Triplet Excited States as Organic Triplet Sensitizers for Triplet-Triplet Annihilation Upconversion. *RSC Adv.* **2012**, *2*, 3942–3953.

(28) Nastasi, F.; Puntoriero, F.; Campagna, S.; Diring, S.; Ziessel, R. Photoinduced Intercomponent Processes in Multichromophoric Species Made of Pt(II)-Terpyridine-Acetylide and Dipyrrromethene-BF₂ Subunits. *Phys. Chem. Chem. Phys.* **2008**, *10*, 3982–3986.

(29) Kim, J. H.; Deng, F.; Castellano, F. N. High Efficiency Low-Power Upconverting Soft Materials. *Chem. Mater.* **2012**, *24*, 2250–2252.

(30) Schulze, T. F.; Czolk, J.; Cheng, Y. Y.; Fockel, B.; MacQueen, R. W.; Khoury, T.; Crossley, M. J.; Stannowski, B.; Lips, K.; Lemmer, U.; Colsmann, A.; Schmidt, T. W. Efficiency Enhancement of Organic and Thin-Film Silicon Solar Cells with Photochemical Upconversion. *J. Phys. Chem. C* **2012**, *116*, 22794–22801.

(31) Cheng, Y. Y.; Fockel, B.; MacQueen, R. W.; Khoury, T.; Clady, R.; Schulze, T. F.; Ekins-Daukes, N. J.; Crossley, M. J.; Stannowski, B.; Lips, K.; Schmidt, T. W. Improving the Light-Harvesting of Amorphous Silicon Solar Cells with Photochemical Upconversion. *Energy Environ. Sci.* **2012**, *5*, 6953–6959.

(32) Chen, H. C.; Hung, C. Y.; Wang, K. H.; Chen, H. L.; Fann, W. S.; Chien, F. C.; Chen, P. L.; Chow, T. J.; Hsu, C. P.; Sun, S. S. White-Light Emission from an Upconverted Emission with an Organic Triplet Sensitizer. *Chem. Commun.* **2009**, 4064–4066.

(33) Singh-Rachford, T. N.; Islangulov, R. R.; Castellano, F. N. Photochemical Upconversion Approach to Broad-Band Visible Light Generation. *J. Phys. Chem. A* **2008**, *112*, 3906–3910.

(34) Wu, W.; Guo, H.; Wu, W.; Ji, S.; Zhao, J. Organic Triplet Sensitizer Library Derived from a Single Chromophore (BODIPY) with Long-Lived Triplet Excited State for Triplet–Triplet Annihilation Based Upconversion. *J. Org. Chem.* **2011**, *76*, 7056–7064.

(35) Lambert, C. R.; Kochevar, I. E. Electron Transfer Quenching of the Rose Bengal Triplet State. *Photochem. Photobiol.* **1997**, *66*, 15–25.

(36) Demas, J. N.; Crosby, G. A. Measurement of Photoluminescence Quantum Yields: Review. *J. Phys. Chem.* **1971**, *75*, 991–1024.

(37) Olmsted, J. Calorimetric Determinations of Absolute Fluorescence Quantum Yields. *J. Phys. Chem.* **1979**, *83*, 2581–2584.